Deep-level photoluminescence due to dislocations and oxygen precipitates in multicrystalline Si

Michio Tajima,[1,2,a)] Yasuaki Iwata,[1] Futoshi Okayama,[1,2] Hiroyuki Toyota,[1] Hisashi Onodera,[3] and Takashi Sekiguchi[3]
[1]*Institute of Space and Astronautical Science/JAXA, Sagamihara 252-5210, Japan*
[2]*Meiji University, Kawasaki 214-8571, Japan*
[3]*National Institute for Materials Science, Tsukuba 305-0044, Japan*

(Received 17 February 2012; accepted 10 May 2012; published online 11 June 2012)

We have demonstrated the presence of a dislocation-related component and a component due to oxygen precipitates in a broad deep-level photoluminescence (PL) band in multicrystalline Si at room temperature. In PL intensity mapping, the lower-energy side of the deep-level PL band at about 0.79 eV appeared as a dark line along a small-angle grain boundary (SA-GB) surrounded by a bright band on either side, while the higher-energy side at about 0.87 eV as a bright line along the SA-GB. These intensity variations agree with the low-temperature PL intensity patterns for well-established dislocation-related lines of D1/D2 and those for oxygen precipitates, respectively. These patterns were observed around SA-GBs with a misorientation angle of 1–2°, and were assumed to be due to the distribution of secondary defects or impurities trapped by the strain field around dislocation clusters forming SA-GBs and that of preferential oxygen precipitation on the dislocations. A spectral component associated with the D3/D4 lines was also extractable from the deep-level PL at about 0.94 eV. The intensity increased on SA-GBs with the angle of $<1°$, where oxygen precipitation did not occur. This corresponds to the generally accepted idea that the D3/D4 lines are related to the intrinsic nature of dislocations. © *2012 American Institute of Physics*. [http://dx.doi.org/10.1063/1.4728194]

I. INTRODUCTION

Multicrystalline Si (mc-Si) is a promising material for mass production of high-efficiency solar cells. The conversion efficiency of the mc-Si cells is, however, lower than that of single crystalline Si (sc-Si) cells. This is due to the reduction of the minority carrier lifetime because of the carrier recombination at the intragrain defects. Dislocation clusters forming small-angle grain boundaries (SA-GBs) are known to become harmful recombination centers after decoration with metallic or oxygen impurities.[1–3] Oxygen impurities, unlike metallic impurities, are difficult to be eliminated by the segregation effect. Although there are some cases where the oxygen concentration is lower than the solubility limit, preferential precipitations on dislocations are unavoidable. Therefore, the accurate analysis of dislocations and oxygen precipitates will be one important issue for the improvement of mc-Si solar cells.

Imaging of band-edge (BE) photoluminescence (PL) at room temperature is regarded as one of the most useful techniques for evaluating the quality of wafers for solar cells,[4] because the intensity is proportional to the minority carrier lifetime and recombination centers originating from intragrain defects appear as dark spots and lines.[4–7] In contrast, less attention has been paid to deep-level PL from mc-Si wafers, particularly at room temperature. Sharp PL lines at 0.81, 0.88, 0.93, and 1.00 eV at low temperatures, termed D1, D2, D3, and D4, respectively, are the well-characterized deep-level PL associated with dislocations in sc-Si,[8–10] and were also observed in mc-Si.[5–7] However, the origin of D lines has not yet been definitely clarified. A featureless broad band appeared with a peak around 0.8 eV at room temperature and its correlation with the D-lines has been discussed.[5,6,11] Appearance of multiple deep-level bands around 0.8 eV was reported in electroluminescence (EL) from mc-Si solar cells and its correlation with grain boundaries was discussed.[12] We also observed deep-level PL at about 0.78 eV in annealed sc-Si (Ref. 13) and later in mc-Si involving SA-GBs at room temperature,[14] and identified its origin as oxygen precipitates, differentiating it from the D lines. The idea was supported by Binetti *et al.*[15] in their PL experiment and by Bothe *et al.*[16] in their EL experiment.

In this paper, we revisit our previous results of deep-level PL in sc-Si and mc-Si and make a comprehensive survey of deep-level PL at 7–295 K. We modify our previous identification and re-assign the multiple components of deep-level PL on the basis of detailed microscopic and monochromatic PL mapping around SA-GBs in mc-Si. We will demonstrate the usefulness of deep-level PL at room temperature. The paper is organized as follows: Measured samples and the apparatus and conditions for PL measurements are described in Sec II. Section III is results and discussion: First, we survey the deep-level PL spectra in mc-Si in Sec. III A, then we show intensity mapping of respective PL components around characteristic SA-GBs in Sec. III B. Finally, the behavior of oxygen precipitation is discussed in Sec. III C. In Sec. IV, our perspective of deep-level PL in mc-Si is given in relation to dislocations and oxygen precipitation.

a)E-mail: tajima@isas.jaxa.jp.

II. EXPERIMENTAL TECHNIQUE

Samples used in this study were mc-Si wafers sliced from ingots grown by a unidirectional solidification method. The slicing damage was etched off by a HNO_3/HF solution. We focused on a p-type B-doped sample with a resistivity of about 2.5 Ω·cm and oxygen and carbon concentrations of about 1×10^{17} and $1–3 \times 10^{17}$ cm^{-3}, respectively, where the oxygen and carbon concentrations were obtained by Fourier transform infrared spectroscopy for a 2 mm thick wafer adjacent to the wafer for PL measurement. The sample contained SA-GBs forming a characteristic loop, around which we had previously analyzed deep-level PL in detail.[14] The crystallographic orientation was measured with an electron backscatter diffraction (EBSD) apparatus under an acceleration voltage of 25 kV. We also used other mc-Si wafers from different suppliers to demonstrate the generality of our findings.

PL spectroscopy and mapping were performed at 15–300 K under the excitation of the 532 nm line of an Nd:YVO_4 laser. The sample was mounted on a cryostat of a He closed-cycle type for low-temperature measurements. PL intensity mappings were taken by scanning the wafer with respect to a laser beam at room temperature and by scanning a laser beam on the wafer surface at low temperatures. The beam diameter was about 10 μm for both temperatures, while the interval of data sampling was 2 and 10 μm for room and low temperatures, respectively. Emission from the sample was passed through bandpass filters to extract specific spectral components of interest, and then detected by a cooled photomultiplier (Hamamatsu R5509-72) and Ge *pin* diode (Northcoast EO-817P) for room and low temperatures, respectively. Details of the mapping apparatuses for room and low temperatures were described previously.[17,18] In PL intensity mappings in Figs. 2, 4, 5, and 6, whiter regions indicate higher intensity, where different minimum to maximum scalings are used to enhance the contrast. We will focus on PL intensity patterns and not discuss the intensity contrast quantitatively, because the intensity is influenced by many factors, such as the overlapping of multiple components, the transmission range of the bandpass filters, the background noise level, and the detector sensitivity. The spatial resolution of the present technique was determined by the volume of the photo-excitation, the diffusion of photo-excited carriers and the spatial filter of the mapping apparatus, and was estimated to be about a few tens μm. The resolution became higher at a defective area because of the reduction of the diffusion length in that area.

Temperature-variable PL spectroscopy was performed under the 532 nm excitation with a beam diameter of about 3 mm. Emission from the sample was dispersed by a monochromator (Photon design PDP320: $f = 0.32$ m) with a 300 groove/mm grating blazed at 1.0 μm, and detected by a cooled InGaAs photodiode array (Princeton Instruments OMA V) with a spectral resolution of 4.8 nm in the wavelength region between 1000 and 1650 nm. For microscopic PL spectroscopy at room temperature, we transferred the optical signal at the point of interest in mapping to the monochromator by an optical fiber. The spectral response of the measurement system was calibrated with blackbody radiation for temperature-variable PL spectroscopy but not for microscopic PL spectroscopy at room temperature.

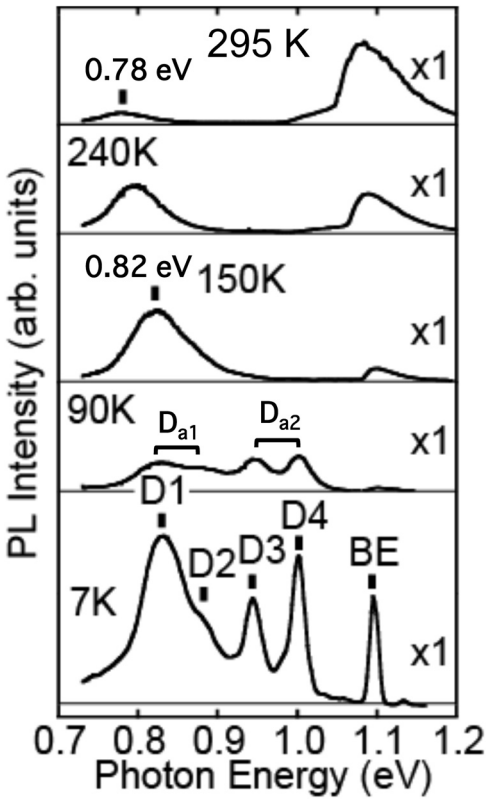

FIG. 1. Temperature dependence of PL spectra in area involving SA-GBs in mc-Si.

III. RESULTS AND DISCUSSION

A. Deep-level PL spectroscopy

First, we surveyed the spectral components of deep-level PL from mc-Si. Multiple components were observed in the PL spectra at 7–295 K, as shown in Fig. 1, where the spectra were taken macroscopically with an excitation beam of 3 mm on the area involving SA-GBs. Figure 2(a) is the microscopic intensity mapping of the BE emission at room

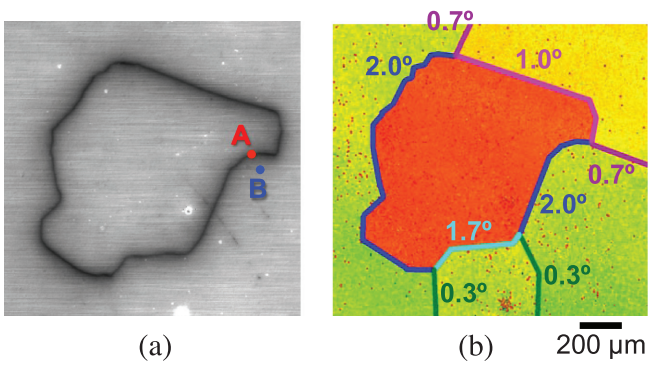

FIG. 2. (a) Intensity mapping of BE-PL at room temperature in area involving SA-GBs in mc-Si. PL spectra were taken microscopically on and near off SA-GB as marked by circles A and B, respectively, using a 10 μm diameter beam excitation. (b) EBSD image of the same area as (a). Misorientation angles of SA-GBs are appended to boundary lines.

temperature on the measured area, indicating the presence of a loop-like dark line. The loop was identified as being due to SA-GBs from the EBSD measurement on the identical part as shown in Fig. 2(b): Misorientation angles of the SA-GBs are appended to boundary lines with an accuracy of $\pm 0.4°$. It should be noted that the dark-line pattern appeared for SA-GBs with a misorientation angle $\geq 1°$. We believe that the pattern is the cross section of the columnar structure of SA-GBs.[7] We will discuss the nature of the SA-GBs in relation to their misorientation angles later in this paper.

The D1-D4 lines dominated the deep-level PL at 7 K. With increasing temperature, their intensities were reduced and D1/D2 and D3/D4 lines were merged into broad bands D_{a1} and D_{a2}, respectively, at 90 K. At 150 K, a very broad band appeared with a peak around 0.82 eV. This spectral change was reported previously[14] and a similar spectral change was also observed in sc-Si.[13] We explained at that time that the 0.82 eV band consisted of the D_{a1} and D_{a2} bands and a new band termed D_b. Our previous understanding[13,14] was that the D_{a1} and D_{a2} bands were decreased with temperature and that only the D_b band remained at room temperature, where the peak was shifted to 0.78 eV in parallel with the band-edge narrowing due to the temperature rise. In sc-Si, the 0.78 eV band at room temperature was identified as being due to oxygen precipitates on the basis of its correlation with the concentration of the precipitated oxygen.[19,20]

In order to check this idea, we took PL spectra microscopically on and near off a SA-GB as marked by circles A and B, respectively, in Fig. 2(a), using a 10 μm diameter beam excitation. The spectra from the two points indicate a substantial difference, as shown in Fig. 3: The intensity of the higher energy region of the deep-level PL is apparently stronger on the SA-GB (point A) than that off the SA-GB (point B). This suggests the presence of multiple components in the featureless broad PL band at room temperature as opposed to our previous hypothesis. We, therefore, realized the necessity of performing monochromatic mapping of deep-level PL at various temperatures.

B. Monochromatic mapping of deep-level PL

As reviewed in Sec. III A, there have been observed seven deep-level PL components: D1-D4 lines, D_{a1} and D_{a2} band, and D_b band. Similarities in optical properties between D1 and D2 lines and those between D3 and D4 have been pointed out by many researchers.[9,10,21,22] We also found the similarities in their intensity patterns in the present sample at 15 K. The D_{a1} and D_{a2} bands have the same origin as the D1/D2 and D3/D4 lines, respectively, as reported previously.[13,14] Therefore, the seven components were categorized into three groups of the D1 (D_{a1}), D_b, and D3 (D_{a2}) components. In the following part, we show monochromatic mapping at three photon energy regions around 0.79, 0.87, and 0.94 eV for monitoring the D1 (D_{a1}), D_b, and D3 (D_{a2}) components, together with the BE component at about 1.1 eV. We used band-pass filters with transmission ranges of 0.79 ± 0.01, 0.875 ± 0.015, and 0.935 ± 0.025 eV for monitoring the three bands. In fact, we took PL mappings using various band-pass filters with transmission ranges from 0.78 to 1.00 eV and found that the above three transmission ranges represented the essential features of the deep-level PL components with little effect of overlapping of neighboring components.

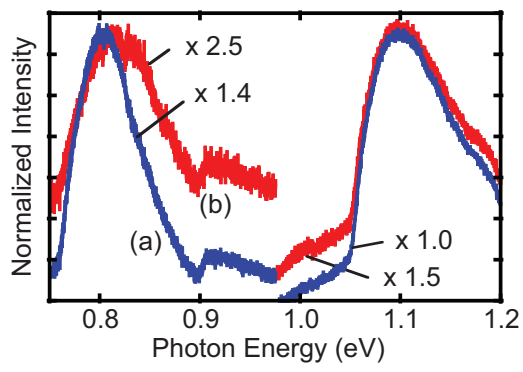

FIG. 3. PL spectra (a) on SA-GB and (b) near off SA-GB, circles A and B in Fig. 2(a), respectively, in mc-Si at 295 K. Symbol "×2.5" denotes amplitude factor.

The intensity mappings of D1, D3, and BE emission at 15 K are shown in Figs. 4(i), 4(j), and 4(k), respectively. It should be noted that the D1 line appeared as a bright loop-like band with a dark core as shown in Fig. 4(i), where the core region corresponds to the dislocation clusters forming SA-GBs with a misorientation angle of 1–2°. This is consistent with the previous report on the D1/D2 line mapping on sc-Si crystals,[13,22] and supports the idea that the D1/D2 lines originate in secondary defects or impurities trapped by the strain field around the dislocations.[10,22] In contrast, the D3 line appeared as a dark loop as shown in Fig. 4(j). This contradicts previous findings in sc-Si that the D3/D4 lines are intrinsic to dislocations and are strong on the dislocations.[13,21,22] This will be discussed later. It should be pointed out that several bright lines were linked radially from the dark loop, corresponding to the SA-GBs with a misorientation angle $<1°$ (Fig. 2(b)).

As the temperature was raised above 150 K, the deep-level PL band became broad and featureless, as shown in Fig. 1. However, the intensity pattern of the three components showed a striking difference. We mapped the intensity at 0.79, 0.87, and 0.94 eV at 150 K in Figs. 4(e)–4(g). The intensity mappings at 0.79 and 0.94 eV showed patterns similar to D1 (D_{a1}) and D3 (D_{a2}), respectively. In contrast, the mapping at 0.87 eV showed a loop-like bright line, which was obviously different from either the D1 (D_{a1}) or D3 (D_{a2}) pattern. This is the characteristic of the intensity pattern for the D_b band and is the basis for the hypothesis that the band is due to the oxygen precipitates, since the oxygen precipitation occurs preferentially on dislocation clusters forming SA-GBs. This intensity contrast was reported previously[14] and was also observed in sc-Si.[13] It should be noted that the D_b band could not be observed below 100 K. The intensity pattern at 0.87 eV was essentially the same as that of the D1 line, which corresponds to the fact that the D2 line with a peak at 0.88 eV is the dominant spectral component at 0.87 eV below 100 K.

Almost the same intensity patterns were observed for the three components at room temperature, as shown in Figs.

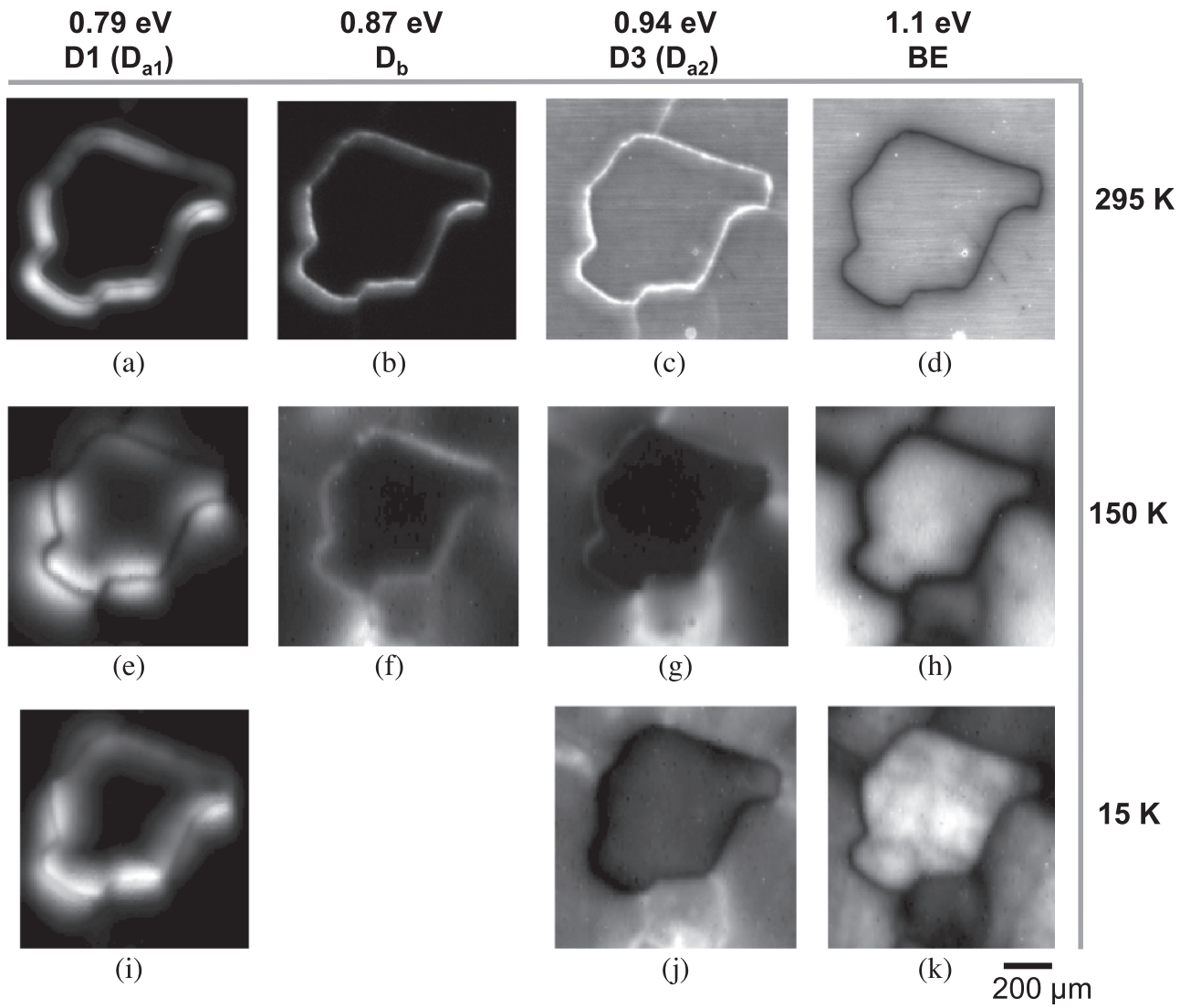

FIG. 4. PL intensity mappings of 0.79, 0.87, 0.94, and 1.1 eV components, representing D1 (D_{a1}), D_b, D3 (D_{a2}) and BE bands, respectively, on mc-Si wafer at 15, 150, and 295 K. Whiter regions indicate higher PL intensity. Intensity contrast is not the same among (a)-(k).

4(a)–4(c). The intensity contrast of the loop pattern at 0.94 eV (Fig. 4(c)) was, however, different from that for the D_{a2} band at 150 K (Fig. 4(g)): bright at room temperature but dark at 150 K. We believe that the overlapping of the tail of the strong D_b band enhanced the intensity along the loop at room temperature. The intensity contrast of the radial line pattern linked from the loop, which corresponded to SA-GBs with angles of 0.3° and 0.7° in Fig. 2(b), was similar among 15, 150, and 295 K, as shown in Figs. 4(j), 4(g), and 4(c). From these, we conclude that the deep-level emission at room temperature includes the dislocation-related D_{a1} and D_{a2} components together with the D_b component due to oxygen precipitates. In our previous report,[14] we recognized only the 0.87 eV component (the D_b band) and overlooked the presence of the other components at room temperature. The 0.87 eV component is emitted only from the core region of SA-GBs, while the 0.79 eV component from the broad band on either side of the core: The 0.79 eV component area is thus apparently wider than the 0.87 eV component area. This is the reason why the macroscopic PL spectra at room temperature in Fig. 1 were dominated by the 0.79 eV component.

We investigated the generality of the present findings by measuring the intensity patterns of the three deep-level components on two other mc-Si samples from different suppliers. The microscopic intensity patterns for the 0.79, 0.87, and 0.94 eV bands together with the BE emission at 1.1 eV are shown in Fig. 5. The same characteristics of the intensity patterns were observed for the three components: The 0.79 eV component appeared as dark lines along the SA-GBs surrounded by a bright band on either side, while the 0.87 eV component as bright lines on the SA-GBs. Extra bright lines were observed for the 0.94 eV component together with the pattern similar to the 0.87 eV component.

C. Oxygen precipitation on SA-GBs

It is interesting to point out that the loop pattern of the D_b band appears granular, as shown in Fig. 6, where the upper part of Fig. 4(b) is enlarged. We believe that this

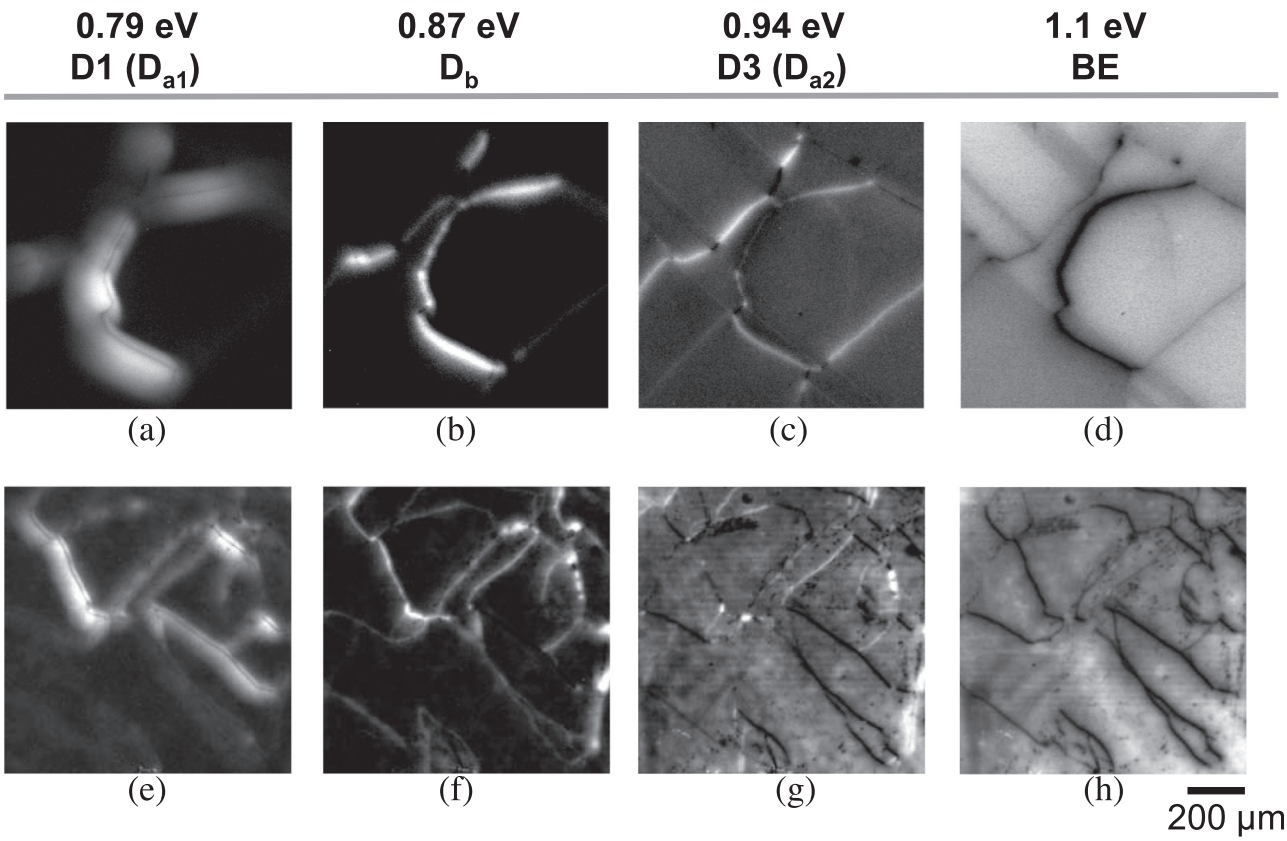

FIG. 5. PL intensity mappings of 0.79, 0.87, 0.94, and 1.1 eV components at 295 K, representing D_{a1}, D_b, D_{a2}, and BE bands, respectively, on two mc-Si wafers from different suppliers. Whiter regions indicate higher PL intensity. Intensity contrast is not the same among (a)-(h).

reflects the precipitation behavior of oxygen on dislocations.[16,23,24] Comparison between Figs. 2(b) and 4(b) indicates that the oxygen precipitation occurs strongly on SA-GBs with a misorientation angle of 1–2°. This may correlate with the strong electronic activity of electron beam induced current signal on SA-GBs with an angle of 2°.[25] We speculate that the intrinsic properties of dislocations are hindered by the oxygen precipitation. This might be the reason that the D3/D4 lines did not become strong along the loop (Fig. 4(g)). In fact, the D3/D4 and D_{a2} bands became strong on the lines linked with the loop, in which the misorientation angle was less than 1° and no oxygen precipitation occurred.

The intensity of the 0.87 eV component along a SA-GB has a positive correlation with that of the 0.79 eV component in the surrounding band on either side of the SA-GB. This is explained as follows: A high intensity area of the 0.87 eV component represents heavy oxygen precipitation. The precipitation induces a large strain field, through which secondary defects or impurities are trapped, resulting in the high intensity of the 0.79 eV component in the surrounding area. This may explain the correlation between the intensity of the 0.78 eV band and precipitated oxygen concentration in sc-Si,[19,20] although the correlation has not yet been examined in mc-Si.

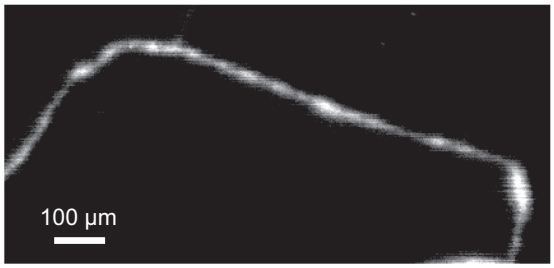

FIG. 6. PL intensity mapping of deep-level emission at 0.87 eV associated with oxygen precipitates at 295 K (Enlarged illustration of upper part of Fig. 4(b)). Whiter regions indicate higher PL intensity.

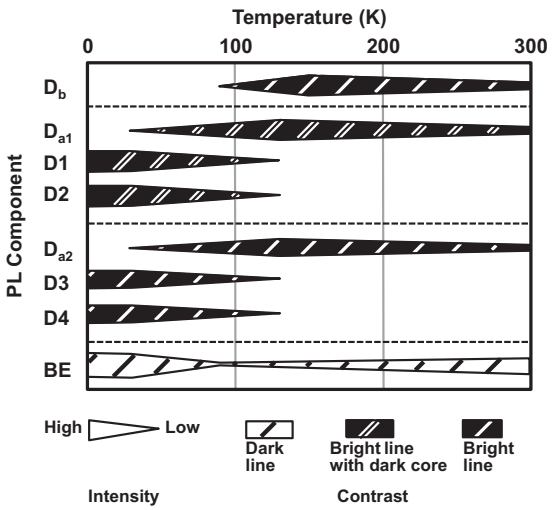

FIG. 7. Schematic chart of intensity variations of D1-D4, D_b, D_{a1}, D_{a2}, and BE emissions depending on sample temperature. Bar width represents PL intensity, and bar pattern distinguishes intensity contrast around SA-GBs.

IV. CONCLUSION

We surveyed the deep-level PL emission in the region containing SA-GBs in mc-Si at temperatures from 7 to 295 K. The results are schematically summarized in Fig. 7, where bar widths represents the intensities, and the bar patterns distinguish the intensity contrast around SA-GBs. Dislocation-related lines D1-D4 appeared dominantly at temperatures below 90 K. The D1 and D2 lines and the D3 and D4 lines merged into the D_{a1} and D_{a2} band, respectively, at >90 K. As the temperature was raised above 150 K, the deep-level PL became one featureless broad band and was observable up to room temperatures. We showed the presence of multiple components in the broad band on the basis of the microscopic intensity variations of respective spectral components around SA-GBs. The D_{a1} (D1/D2) component at 0.79 eV appeared as a dark line along an SA-GB with a misorientation angle of 1–2° surrounded by a bright band on either side, while the D_b component at 0.87 eV appeared as a bright line along the SA-GB. These patterns correspond with the distribution of secondary defects or impurities trapped by the strain field around dislocation clusters forming SA-GBs and that of preferential oxygen precipitation on the dislocations, respectively, reflecting the origins of the D_{a1} (D1/D2) and D_b bands. These characteristic patterns were not observed for SA-GBs with an angle of <1°. This leads us to suggest that oxygen precipitation proceeds on SA-GBs with an angle of 1–2°. The D_{a2} (D3/D4) component at 0.94 eV appeared as a bright line on an SA-GB with an angle of <1°. This is consistent with the fact that the D3/D4 (D_{a2}) band reflects the intrinsic nature of dislocations: The oxygen precipitation hinders the nature in SA-GBs with an angle of 1–2°. We believe that the present systematic spectral changes and intensity-pattern variations are general in the region involving SA-GBs in mc-Si, since essentially the same results were obtained in multiple samples from different suppliers.

ACKNOWLEDGMENTS

The authors would like to thank Professors A. Ogura, Y. Ohshita, and K. Arafune for the preparation of the sample and for useful discussion and comments, Mr. M. Inoue for his help in the interpretation of the data in Ref. 4, and Dr. F. Yin for the EBSD measurement. This work was partly supported by the New Energy and Industrial Technology Development Organization (NEDO) under the Ministry of Economy, Trade and Industry (METI).

[1]W. Seifert, G. Morgenstern, and M. Kittler, Semicond. Sci. Technol. **8**, 1687 (1993).
[2]H. J. Möller, L. Long, M. Werner, and D. Yang, Phys. Stat. Sol. A **171**, 175 (1999).
[3]B. Sopori, P. Rupnowski, V. Mehta, V. Budhraja, S. Johnston, N. Call, H. Mountinho, M. Al-Jassim, A. Shaikh, M. Seacrist, and D. Carlson, ECS Trans. **18**, 1049 (2009).
[4]T. Trupke, R. A. Bardos, M. C. Schubert, and W. Warta, Appl. Phys. Lett. **89**, 044107 (2006).
[5]S. Ostapenko, I. Tarasov, J. P. Kalejs, C. Haessler, and E.-U. Reisner, Semicond. Sci. Technol. **15**, 840 (2000).
[6]M. Kittler, W. Seifert, T. Arguirov, I. Tarasov, and S. Ostapenko, Sol. Energy Mater. Sol. Cells **72**, 465 (2002).
[7]H. Sugimoto, M. Inoue, M. Tajima, A. Ogura, and Y. Ohshita, Jpn. J. Appl. Phys. **45**, L641 (2006).
[8]N. A. Drozdov, A. A. Partin, and V. D. Tkachev, Sov. Phys.-JETP Lett. **23**, 597 (1976).
[9]M. Suezawa, Y. Sasaki, Y. Nishina, and K. Sumino, Jpn. J. Appl. Phys. **20**, L537 (1981).
[10]R. Sauer, J. Weber, J. Stolz, E.R. Weber, K.-H. Küsters, and H. Alexander, Appl. Phys. A **36**, 1 (1985).
[11]T. Mchedlidze, O. Kononchuk, T. Arguirov, M. Trushin, M. Reiche, and M. Kittler, Solid State Phenom. **156–158**, 567 (2010).
[12]F. Dreckschmidt and H. J. Möller, Phys. Status Solidi C **8**, 1356 (2011).
[13]M. Tajima, M. Tokita, and M. Warashina, Mater. Sci. Forum **196–201**, 1749 (1995).
[14]M. Inoue, H. Sugimoto, M. Tajima, Y. Ohshita, and A. Ogura, J. Mater. Sci. Mater. Electron. **19**, S132 (2008).
[15]S. Binetti, S. Pizzini, E. Leoni, R. Somaschini, A. Castaldini, and A. Cavallini, J. Appl. Phys. **92**, 2437 (2002).
[16]K. Bothe, K. Ramspeck, D. Hinken, C. Schinke, J. Schmidt, S. Herlufsen, R. Brendel, J. Bauer, J.-M. Wagner, N. Zakharov, and O. Breitenstein, J. Appl. Phys. **106**, 104510 (2009).
[17]M. Tajima, Z. Li, and R. Shimidzu, Jpn. J. Appl. Phys. **41**, L1505 (2002).
[18]M. Tajima, in *Proceedings of Defect Recognition and Image Processing in Semiconductors 1995 (DRIP VI)*, Estes Park, CO [Inst. Phys. Conf. Ser. **149**, 243 (1996)].
[19]M. Tajima, H. Takeno, and T. Abe, "Defects in Semiconductors 16," in *Materials Science Forum*, edited by G. Davies, G. G. DeLeo, and M. Stavola (Trans Tech Publications, Switzerland, 1991), Vol. 83–87, p. 1327.
[20]Y. Kitagawara, R. Hoshi, and T. Takenaka, J. Electrochem. Soc. **139**, 2277 (1992).
[21]T. Sekiguchi and K. Sumino, J. Appl. Phys. **79**, 3253 (1996).
[22]E. C. Lightowlers and V. Higgs, Phys. Status Solidi A **138**, 665 (1993).
[23]H. Nordmark, M. Di Sabatino, M. Acciarri, J. Libal, S. Binetti, E. J. Ovrelid, J. Walmsley, and R. Holmestad, in Proceedings of 33rd IEEE Photovoltaic Specialists Conference, San Diego, California, 11–16 May 2008.
[24]S. Binetti, J. Libal, M. Acciarri, M. Di Sabatino, H. Nordmark, E. J. Øvrelid, J. C. Walmsley, and R. Holmestad, Mater. Sci. Eng. B **159–160**, 274 (2009).
[25]J. Chen and T. Sekiguchi, Jpn. J. Appl. Phys. **46**, 6489 (2007).